JACS
JOURNAL OF THE AMERICAN CHEMICAL SOCIETY
pubs.acs.org/JACS
Article

Introducing Frustrated Lewis Pairs to Metal−Organic Framework for Selective Hydrogenation of *N*-Heterocycles

Ze-Ming Xu, Zhuoyi Hu, Yali Huang, Shu-Jin Bao, Zheng Niu,* Jian-Ping Lang,* Abdullah M. Al-Enizi, Ayman Nafady, and Shengqian Ma*

Cite This: *J. Am. Chem. Soc.* 2023, 145, 14994−15000
Read Online
ACCESS | Metrics & More | Article Recommendations | Supporting Information

ABSTRACT: Hydrogenated nitrogen heterocyclic compounds play a critical role in the pharmaceutical, polymer, and agrochemical industries. Recent studies on partial hydrogenation of nitrogen heterocyclic compounds have focused on costly and toxic precious metal catalysts. As an important class of main-group catalysts, frustrated Lewis pairs (FLPs) have been widely applied in catalytic hydrogenation reactions. In principle, the combination of FLPs and metal−organic framework (MOF) is anticipated to efficiently enhance the recyclability performance of FLPs; however, the previously studied MOF-FLPs showed low reactivity in the hydrogenation of *N*-heterocycles compounds. Herein, we offer a novel P/B type MOF-FLP catalyst that was achieved via a solvent-assisted linker incorporation approach to boost catalytic hydrogenation reactions. Using hydrogen gas under moderate pressure, the proposed P/B type MOF-FLP can serve as a highly efficient heterogeneous catalyst for selective hydrogenation of quinoline and indole to tetrahydroquinoline and indoline-type drug compounds in high yield and excellent recyclability.

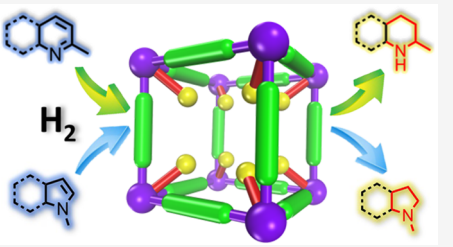

INTRODUCTION

Selective hydrogenation of nitrogen heterocyclic molecules is one of the most important transformations in organic synthesis for the production of various compounds in the pharmaceutical, polymer, and agrochemical industries.[1] In the past decades, a variety of precious metal catalysts have been extensively utilized in the selective hydrogenation of nitrogen heterocyclic molecules.[2] However, the high cost of precious metal catalysts and their toxicity have limited their widespread use in industry and in other catalytic transformations. Alternatively, the studies on metal-free hydrogenation catalysts have recently attracted increasing interest due to their potential low cost and weak toxicity.[3] As one of the important main-group catalysts, frustrated Lewis pairs (FLPs) have been applied in the partial hydrogenation of various nitrogen heterocyclic compounds, such as quinolines, indoles, and phenanthrolines in homogeneous reactions.[4] However, compared with pervasive heterogeneous catalysts, most FLPs serve as hydrogenation catalysts in the homogeneous reaction systems and lose their activation after completion of the reactions, thereby limiting their possible utility. Therefore, developing heterogeneous FLP catalysts with excellent recyclability and great catalytic reduction performance of nitrogen heterocyclics is highly desirable yet challenging.

As an emerging class of crystalline porous materials, metal−organic frameworks (MOFs) have been extensively employed in heterogeneous catalysis, benefiting from their structural diversity and tailorability.[5] The integration of MOFs with a catalytic center endows the MOF-based heterogeneous catalyst with excellent recycling performance and special selectivity.[6,7] In recent years, some research efforts have been devoted to grafting N/B type FLPs onto MOFs to construct novel heterogeneous catalysts.[8] In 2019, we reported the chemoselectively hydrogenate α,β-unsaturated imine to the corresponding amine using MIL-101(Cr)-FLP-H_2 as a heterogeneous catalyst,[9] in which the DABCO and $B(C_6F_5)_2(Mes)$ exhibited as frustrated Lewis pairs to tailor the pore environment. However, the N/B type MOF-FLP heterogeneous catalyst showed unsatisfactory catalysis performance in the hydrogenation of nitrogen heterocyclic compounds since the lower Lewis acidity of $B(C_6F_5)_2(Mes)$ leads to low reactivity (Scheme 1, Supporting Information). Compared with N/B type FLP, P/B type FLP has gained marked interest due to its outstanding performance in the hydrogen activation reactions.[4m] Given the difficulty in the synthesis of suitable P-containing Lewis base, caused by its possible oxidation and coordination with the metal node of MOF,[10] the P/B type MOF-FLP has not been developed.

In this work, we designed a P/B type MOF-FLP to explore the selective hydrogenation of nitrogen heterocyclic molecules (Scheme 1). The MOF, NU-1000, $[Zr_6(\mu_3\text{-}O)_4(\mu_3\text{-}$

Received: May 11, 2023
Published: June 29, 2023

https://doi.org/10.1021/jacs.3c04929
J. Am. Chem. Soc. 2023, 145, 14994−15000

Scheme 1. Types of Different MOF-FLPs for *N*-Heterocycles Hydrogenation Reactions

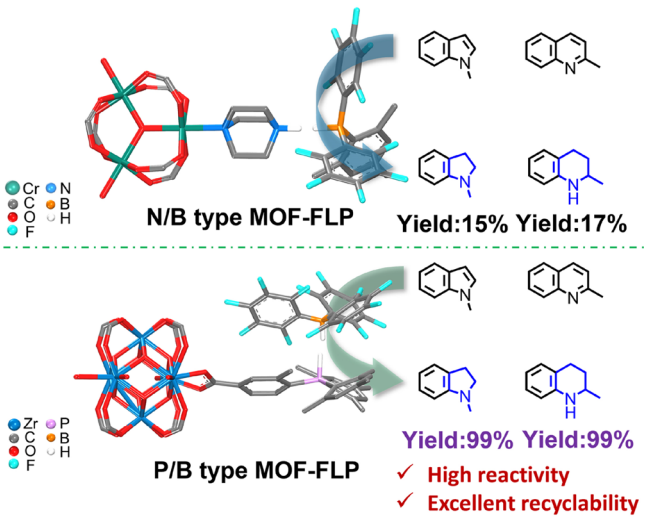

$OH)_4(OH)_4(H_2O)_4(TBAPy)_2]$ (H_4TBAPy is 1,3,6,8-tetrakis-(*p*-benzoic acid)pyrene), was selected as the platform that has the secondary building unit (SBU) in the form of $[Zr_6(\mu_3\text{-}O)_4(\mu_3\text{-}OH)_4(OH)_4(H_2O)_4]^{8+}$. In the 31 Å diameter mesopores of NU-1000, Lewis base $(2,4,6\text{-}Me_3C_6H_2)_2P(2\text{-}Me\text{-}4\text{-}COOHC_6H_3)$ could be anchored by the method called solvent-assisted linker incorporation (SALI) to achieve the NU-1000-LB.[11] Under a H_2 atmosphere and ambient temperature, Lewis acid $B(C_6F_5)_3$ can be anchored into NU-1000-LB, and the resultant NU-1000-FLP-H_2 was achieved, thereby implying the capability to catalyze the hydrogenation of the quinoline and indole to their corresponding tetrahydroquinoline and indoline products. Remarkably, P/B type MOF-FLP showed great recycling performance in the above catalytic reactions. Consequently, the P/B type MOF-FLP was then employed for the efficient synthesis of tetrahydroquinoline and indoline type drug molecules.

RESULTS AND DISCUSSION

NU-1000 was synthesized using a procedure described in the literature.[11d] The compound $(2,4,6\text{-}Me_3C_6H_2)_2P(2\text{-}Me\text{-}4\text{-}COOHC_6H_3)$ was designed and synthesized as the Lewis base (LB) since the carboxylic acid of the LB can be coordinated with the Zr_6 node in 31 Å diameter mesopores of NU-1000, thus making LB strongly anchored in the pores of NU-1000 thereby yielding NU-1000-LB. To investigate the reactivity of the LB and the $B(C_6F_5)_3$ (Lewis acid, LA), the esters of LB and LA were exposed to a hydrogen atmosphere, giving rise to the phosphonium borates $[(2,4,6\text{-}Me_3C_6H_2)_2PH\text{-}(2\text{-}Me\text{-}4\text{-}COOMeC_6H_3)]^+$ $[HB(C_6F_5)_3]^-$, which can be determined by ^{11}B NMR spectroscopy (Supporting Information (SI), Figure S11). Based on the above reaction, the Lewis acid $B(C_6F_5)_3$ was added to NU-1000-LB, and then reacted with H_2 to obtain the $HB(C_6F_5)_3^-/(2,4,6\text{-}Me_3C_6H_2)_2PH(2\text{-}Me\text{-}4\text{-}COOHC_6H_3)^+$ pair anchored into the NU-1000, which was denoted as the NU-1000-FLP-H_2 (Figure 1). NU-1000-FLP-H_2 (0.67 mmol per 1 g of NU-1000 or 2 FLP per unsaturated Zr_6 node of NU-1000) was used in the following characterizations.

To confirm the existence of the Lewis base in the pores of NU-1000, ^{31}P MAS NMR spectroscopy was investigated. As

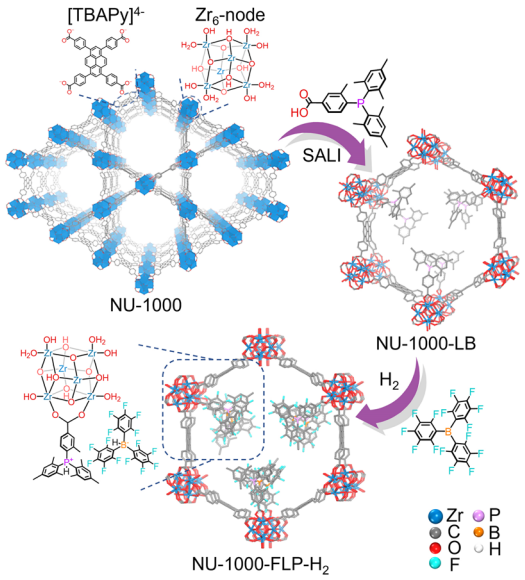

Figure 1. Construction pathway of NU-1000-FLP-H_2.

illustrated in Figure 2a, the solid ^{31}P NMR spectra of NU-1000-LB showed a signal at −28.72 ppm, indicating that the

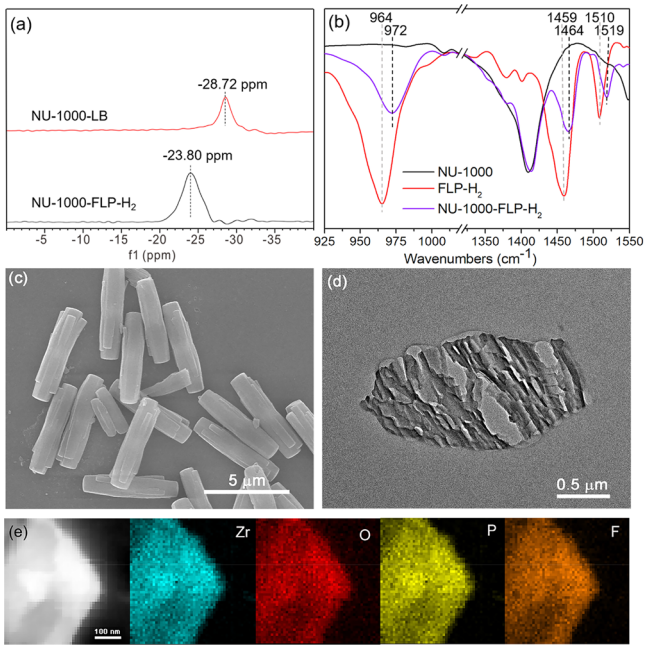

Figure 2. (a) ^{31}P MAS NMR spectra of NU-1000-LB and NU-1000-FLP-H_2. (b) FT-IR spectra of NU-1000, NU-1000-LB, NU-1000-FLP-H_2. (c) SEM image of the NU-1000-FLP-H_2. (d) TEM image and (e) HAADF-STEM image of NU-1000-FLP-H_2 after ultrathin sectioning with the corresponding elemental mapping images.

Lewis base was successfully anchored in NU-1000. After the reaction between $B(C_6F_5)_3$ and NU-1000-LB under hydrogen, a new peak at −23.80 ppm was observed in the solid-state ^{31}P NMR spectrum, which matched well with that of the homogeneous $[(2,4,6\text{-}Me_3C_6H_2)_2PH(2\text{-}Me\text{-}4\text{-}COOMeC_6H_3)]^+[HB(C_6F_5)_3]^-$ ($\delta = -23.28$ ppm), thus confirming the formation of the corresponding FLP-H_2 in the pore of the NU-1000.

https://doi.org/10.1021/jacs.3c04929
J. Am. Chem. Soc. 2023, 145, 14994−15000

The Fourier transform infrared (FT-IR) spectroscopy analysis was employed to confirm the interactions between FLP-H_2 and Zr-clusters on the NU-1000 framework. The characteristic peaks from LB and LA are shown in the IR spectra of NU-1000-FLP-H_2. The new band at 972 cm^{-1} can be attributed to the B−C stretching vibrations of LA, and the other two new bands around 1460 and 1510 cm^{-1} arise from the P-Ph stretching vibrations of LB (Figure 2b). The above bands of NU-1000-FLP-H_2 further confirmed the anchored FLP-H_2 in the MOF.

The nitrogen adsorption/desorption measurements at 77 K and powder X-ray diffraction (PXRD) of NU-1000-LB and NU-1000-FLP-H_2 were, respectively, measured to verify their porosity and phase purity. As shown in Figure S13, the PXRD patterns of NU-1000-LB and NU-1000-FLP-H_2 are in excellent agreement with the patterns of NU-1000, suggesting the framework integrity of NU-1000-FLP-H_2. The N_2 sorption isotherms indicated that the BET surface area of NU-1000-LB and NU-1000-FLP-H_2 decreased to 1554 and 1212 $m^2 \cdot g^{-1}$ compared with parent NU-1000 (SI, Figure S14). Meanwhile, the pore sizes of NU-1000-LB and NU-1000-FLP-H_2 also decreased, which can further confirm that the LB and FLP-H_2 molecules were grafted in the mesopores of NU-1000 (SI, Figure S15).

The SEM image of NU-1000-FLP-H_2 verifies that NU-1000 retains its rectangular crystal throughout the encapsulation process (Figure 2c). To investigate the uniform distribution of FLP-H_2 within the pores of NU-1000, the NU-1000-FLP-H_2 was ultrathinly sectioned (Figure 2d). Subsequently, the ultrathin section of NU-1000-FLP-H_2 was studied by high-angle annular dark-field scanning transmission electron microscopy (HAADF-STEM) and energy dispersive X-ray spectroscopy (EDS) elemental mapping analyses. As presented in Figure 2e, the Zr, O, P, and F elements were uniformly distributed throughout the pores.

The existence of LB and FLP-H_2 in the framework was further illustrated by X-ray photoelectron spectra. The P(2p) spectrum showed the P element within the NU-1000-LB (SI, Figure S21), and the spectra of both F(1s) and P(2p) showed the F and P elements within the NU-1000-FLP-H_2 (SI, Figure S24 and Figure S25). Furthermore, the Zr $3d_{5/2}$ binding energy shifts from 183.1 to 182.8 eV after coordination of Lewis base, and after the Lewis acid installation, it shifts slightly to 183.0 eV (SI, Figure S27). Meanwhile, the binding energy of P 2p shifts from 132.9 to 132.8 eV when FLP-H_2 is formed (SI, Figure S28).

To evaluate the effect of FLP uptake amount on the catalysis performance, a series of MOF-FLP with different FLP-H_2 uptake amounts including NU-1000-FLP-H_2-1 (0.16 mmol FLP-H_2 per 1 g NU-1000) and NU-1000-FLP-H_2-2 (0.33 mmol FLP-H_2 per 1 g NU-1000) were prepared. The loading amounts of FLP-H_2 were determined by ^1H NMR spectroscopy after the samples were dissolved in the 10% D_2SO_4−DMSO-d_6 mixture solvent. To evaluate the catalysis performances of NU-1000-FLP-H_2 catalysts, we chose 2-methylquinoline as a substrate and exposed it to 10 mg of catalyst in toluene at 1 MPa H_2 atmosphere at 60 °C for 24 h. The yield of 2-methyl-1,2,3,4-tetrahydroquinoline increased along with the increase of the FLP-H_2 loading amount in NU-1000 (SI, Table S2). Compared with the catalyst NU-1000-FLP-H_2, the MOF-FLP-H_2 with the lower amount of FLP-H_2, NU-1000-FLP-H_2-2, gave a 68% yield; meanwhile, the lowest uptake amount of FLP-H_2 only afforded a 45% yield. Whereas, the suitable uptake amount of FLP-H_2 loaded NU-1000 exhibited excellent catalytic performance. The control experiments using NU-1000 and NU-1000-LB were also conducted; the desired product could not be detected even after a 72 h reaction time, suggesting NU-1000 and NU-1000-LB are inactive for the 2-methylquinoline reduction reaction. In contrast, the heterogeneous NU-1000-FLP-H_2 showed higher catalytic activity than homogeneous FLP-H_2 (SI, Table S2), which can be attributed to the synergistic effect between the MOF and FLP. The interactions between the Zr-OH of NU-1000 and the nitrogen atom of N-heterocycles could activate the C═N bonds of the substrates,[9,12] thus facilitating the hydrogenation of N-heterocycle substrates.

2-Methylquinoline compounds with different substituted groups were used to investigate the catalysis performance of the heterogeneous NU-1000-FLP-H_2. As summarized in Table 1, the reaction yields catalyzed by NU-1000-FLP-H_2 from

Table 1. NU-1000-FLP-H_2 Catalyzed Hydrogenation of Quinoline[a]

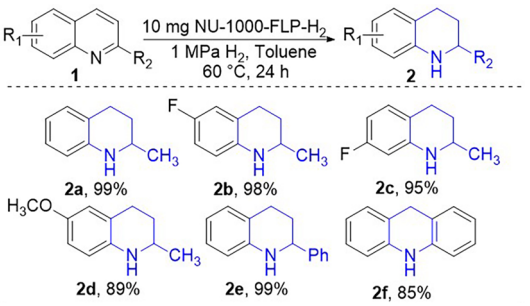

[a]Reaction conditions: 10 mg NU-1000-FLP-H_2, 0.12 mmol **3a**, 2 mL toluene, 1 MPa H_2, 60 °C, 24 h.

related 2-methylquinolines derivatives are 99% for 2-methylquinoline (**2a**), 98% for 6-fluoro-2-methylquinoline (**2b**), 95% for 7-fluoro-2-methylquinoline (**2c**), 89% for 6-methoxy-2-methylquinoline (**2d**), 99% for 2-phenylquinoline (**2e**), and 85% for acridine (**2f**), respectively. In comparison, the yields are 91%, 89%, 84%, 82%, 90%, and 79% when catalyzed by a 5.6 mol % homogeneous FLP-H_2 catalyst, respectively. These results indicate the excellent catalysis performance of porous NU-1000-FLP-H_2 in FLP-promoted hydrogenation. In an effort to further expand the reduction of nitrogen heterocyclic compounds, we further explore the applicability of NU-1000-FLP-H_2 in the partial reduction of 1-methyl-1*H*-indole into 1-methylindoline. As shown in Table 2, the reaction yields catalyzed by NU-1000-FLP-H_2 are 99% for 1-methyl-1*H*-indole (**4a**), 98% for 1,2-dimethyl-1*H*-indole (**4b**), 98% for 1,3-dimethyl-1*H*-indole (**4c**), 95% for 4-bromo-1-methyl-1*H*-indole (**4d**), 99% for 5-chloro-1-methyl-1*H*-indole (**4e**), 85% for 1,7-dimethyl-1*H*-indole (**4f**), 96% for 1,6-dimethyl-1*H*-indole (**4g**), 94% for 6-bromo-1-methyl-1*H*-indole (**4h**), and 97% for 5-methoxy-1-methyl-1*H*-indole (**4i**). These results illustrate that porous NU-1000-FLP-H_2 shows excellent catalysis performance in indole hydrogenation reactions.

To demonstrate the application of NU-1000-FLP-H_2 in the synthesis of drug molecules, a catalytic hydrogen reaction from 2-pentylquinoline (**5**) to 2-pentyl-1,2,3,4-tetrahydroquinoline (**6**) was performed (Figure 3a). In the above hydrogenation reaction, the heteroaromatic ring of quinoline derivative was catalytically reduced. Subsequently, an antimalarial natural

https://doi.org/10.1021/jacs.3c04929
J. Am. Chem. Soc. 2023, 145, 14994−15000

Table 2. NU-1000-FLP-H_2 Catalyzed Hydrogenation of Indole[a]

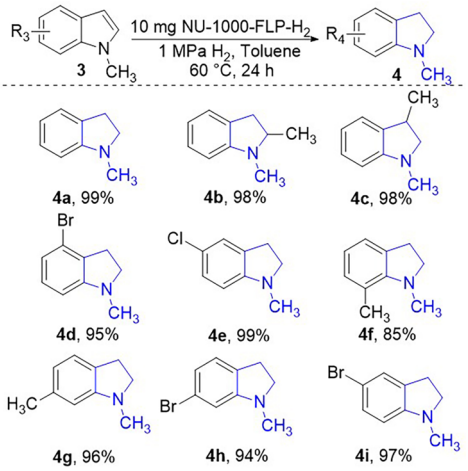

[a]Reaction conditions: 10 mg NU-1000-FLP-H_2, 0.12 mmol **3a**, 2 mL toluene, 1 MPa H_2, 60 °C, 24 h.

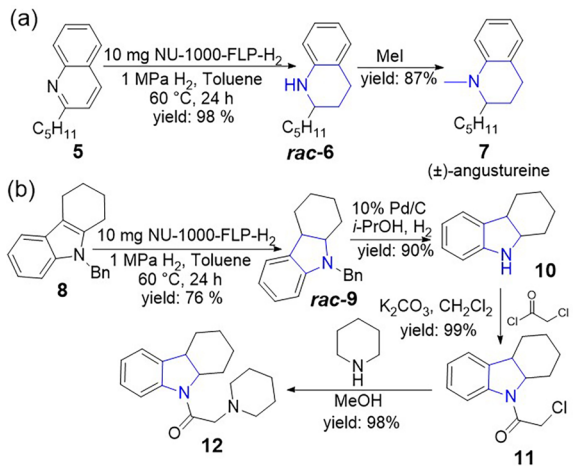

Figure 3. (a) Application of hydrogenation in the synthesis of (±)-angustureine. (b) Synthesis of biologically active product **12**.

product, racemic (±)-angustureine (**7**), was obtained by the methylation of the tetrahydroquinoline derivative. Meanwhile, indoline skeleton derivative **12**, a neuroleptic agent in many types of antidepressants, can also be synthesized by employing NU-1000-FLP-H_2. As depicted in Figure 3b, hydrogenation of indole **8** gave protected racemic hexahydrocarbazole **9** with a 76% yield. The unprotected intermediate hexahydrocarbazole **10** was obtained via the deprotection of **9**. Subsequent protection with 2-chloroacetyl chloride gave intermediate **11**. Finally, *N*-alkylation afforded the racemic biologically active compound **12** in high overall yields.

Based on the homogeneous FLP-H_2 catalyzed hydrogenation reactions, the probable mechanism of NU-1000-FLP-H_2 catalyzed quinoline is proposed in Figure S33.[4l,n,o] This reaction is initiated to proceed via transferring the proton on zwitterion I to quinoline, affording intermediate II, which undergoes nucleophilic attack by the borohydride anion, affording intermediate III and an imine. After that, intermediate III could heterolytically cleave H_2 to obtain intermediate IV. Subsequently, the imine could be hydrogenated to produce V. In the last stage, the zwitterion I could be regenerated via the heterolytic cleavage of H_2.

As a heterogeneous catalyst, the stability and recycling performance of NU-1000-FLP-H_2 were investigated by separating the catalyst via simple centrifuge from the reaction mixture and reusing it in five consecutive runs of the hydrogenation reactions of quinoline and indole. The results indicated that no significant reactivity drop was observed throughout these recycling experiments. The PXRD and N_2 adsorption studies of NU-1000-FLP-H_2 after five cycles further supported the catalysts are robust (SI, Figure S35, Figure S36, and Figure S39 and S40). The SEM (SI, Figure S37a and Figure S41a), TEM (SI, Figure S37b and Figure S41b), and HAADF-STEM images of NU-1000-FLP-H_2 after five cycles indicated the rectangular crystal was still retained. As shown in Figure S37c and Figure S41c, the Zr, P, and F elements were also uniformly distributed.

CONCLUSIONS

In summary, we demonstrated the incorporation of a P/B FLP into NU-1000 to realize the catalytic hydrogenation of *N*-heterocycles by using hydrogen gas. Benefiting from the high hydrogenation activity of the P/B FLP, NU-1000-FLP-H_2 can achieve the hydrogenation of quinolone and indole in high yield with excellent recyclability. Furthermore, NU-1000-FLP-H_2 has been applied in the synthesis of tetrahydroquinoline and indoline-type drug molecules. The findings of this work not only demonstrate the development of new types of efficient MOF-FLP catalysts for some challenging reactions, but also suggest a new route to construct porous FLP-based materials for applications beyond catalysis.

ASSOCIATED CONTENT

Supporting Information

The Supporting Information is available free of charge at https://pubs.acs.org/doi/10.1021/jacs.3c04929.

Experimental procedures, spectroscopic data, and X-ray crystallography (PDF)

AUTHOR INFORMATION

Corresponding Authors

Zheng Niu − *College of Chemistry, Chemical Engineering and Materials Science, Soochow University, Suzhou 215123 Jiangsu, China;* orcid.org/0000-0003-2406-997X; Email: zhengniu@suda.edu.cn

Jian-Ping Lang − *College of Chemistry, Chemical Engineering and Materials Science, Soochow University, Suzhou 215123 Jiangsu, China; State Key Laboratory of Organometallic Chemistry, Shanghai Institute of Organic Chemistry, Chinese Academy of Sciences, Shanghai 200032, China;* orcid.org/0000-0003-2942-7385; Email: jplang@suda.edu.cn

Shengqian Ma − *Department of Chemistry, University of North Texas, Denton, Texas 76201, United States;* orcid.org/0000-0002-1897-7069; Email: Shengqian.Ma@unt.edu

Authors

Ze-Ming Xu − *College of Chemistry, Chemical Engineering and Materials Science, Soochow University, Suzhou 215123 Jiangsu, China*

Zhuoyi Hu − *College of Chemistry, Chemical Engineering and Materials Science, Soochow University, Suzhou 215123 Jiangsu, China*
Yali Huang − *College of Chemistry, Chemical Engineering and Materials Science, Soochow University, Suzhou 215123 Jiangsu, China*
Shu-Jin Bao − *College of Chemistry, Chemical Engineering and Materials Science, Soochow University, Suzhou 215123 Jiangsu, China*
Abdullah M. Al-Enizi − *Department of Chemistry, College of Science, King Saud University, Riyadh 1145, Saudi Arabia;* orcid.org/0000-0002-3967-5553
Ayman Nafady − *Department of Chemistry, College of Science, King Saud University, Riyadh 1145, Saudi Arabia*

Complete contact information is available at: https://pubs.acs.org/10.1021/jacs.3c04929

Notes

The authors declare no competing financial interest.

■ ACKNOWLEDGMENTS

The authors thank the National Natural Science Foundation of China (Grants 22271204 and 22001186), the National Science Foundation of Jiangsu Province (Grant BK20200853), "Distinguished Professor of Jiangsu Province" Program, and the Gusu Innovation Leading Talents Program (Grant Number ZXL2021459), and the State Key Laboratory of Organometallic Chemistry of Shanghai Institute of Organic Chemistry (Grant No. KF2021005 to J.P.L.). Partial support from the Robert A. Welch Foundation (B-0027) is acknowledged (S.M.). The authors also extended their sincere appreciation to Researchers Supporting Program project no. RSP2023R79 at King Saud University, Riyadh, Saudi Arabia for partial support of this work.

■ REFERENCES

(1) (a) Park, S.; Chang, S. Catalytic Dearomatization of *N*-Heteroarenes with Silicon and Boron Compounds. *Angew. Chem., Int. Ed.* **2017**, *56*, 7720−773. (b) Gunasekar, R.; Goodyear, R. L.; Silvestri, I. P.; Xiao, J. Recent Developments in Enantio- and Diastereoselective Hydrogenation of *N*-Heteroaromatic Compounds. *Org. Biomol. Chem.* **2022**, *20*, 1794−1827. (c) Muthukrishnan, I.; Sridharan, V.; Menéndez, J. C. Progress in the Chemistry of Tetrahydroquinolines. *Chem. Rev.* **2019**, *119*, 5057−5191. (d) Trost, B. M.; Fleming, I. *Comprehensive Organic Synthesis*; Pergamon: Oxford, 1991. (e) Siengalewicz, P.; Rinner, U.; Mulzer, J. Recent Progress in the Total Synthesis of Naphthyridinomycin and Lemonomycin Tetrahydroisoquinoline Antitumor Antibiotics (TAAs). *Chem. Soc. Rev.* **2008**, *37*, 2676−2690. (f) Le, V. H.; Inai, M.; Williams, R. M.; Kan, T. Ecteinascidins. A Review of the Chemistry, Biology and Clinical Utility of Potent Tetrahydroisoquinoline Antitumor Antibiotics. *Nat. Prod. Rep.* **2015**, *32*, 328−347.

(2) (a) Wu, J.; Barnard, J. H.; Zhang, Y.; Talwar, D.; Robertson, C. M.; Xiao, J. Robust Cyclometallated Ir(III) Catalysts for the Homogeneous Hydrogenation of *N*-Heterocycles under Mild Conditions. *Chem. Commun.* **2013**, *49*, 7052−7054. (b) Dobereiner, G. E.; Nova, A.; Schley, N. D.; Hazari, N.; Miller, S. J.; Eisenstein, O.; Crabtree, R. H. Iridium-Catalyzed Hydrogenation of *N*-Heterocyclic Compounds under Mild Conditions by an Outer-Sphere Pathway. *J. Am. Chem. Soc.* **2011**, *133*, 7547−7562. (c) Ren, D.; He, L.; Yu, L.; Ding, R.-S.; Liu, Y.-M.; Cao, Y.; He, H.-Y.; Fan, K.-N. Anunusual Chemoselective Hydrogenation of Quinoline Compounds using Supported Gold Catalysts. *J. Am. Chem. Soc.* **2012**, *134*, 17592−17598. (d) Chen, F.; Surkus, A. E.; He, L.; Pohl, M. M.; Radnik, J.; Topf, C.; Junge, K.; Beller, M. Selective Catalytic Hydrogenation of Heteroarenes with *N*-Graphene-Modified Cobalt Nanoparticles (Co_3O_4−Co/NGr@α-Al_2O_3). *J. Am. Chem. Soc.* **2015**, *137*, 11718−11724. (e) Chakraborty, S.; Brennessel, W. W.; Jones, W. D. A Molecular Iron Catalyst for the Acceptorless Dehydrogenation and Hydrogenation of *N*-Heterocycles. *J. Am. Chem. Soc.* **2014**, *136*, 8564−8567. (f) Cho, H.; Török, F.; Török, B. Selective Reduction of Condensed *N*-Heterocycles using Water as a Solvent and a Hydrogen Source. *Org. Biomol. Chem.* **2013**, *11*, 1209−1215.

(3) (a) Gandhamsetty, N.; Joung, S.; Park, S.-W.; Park, S.; Chang, S. Boron-Catalyzed Silylative Reduction of Quinolines: Selective sp^3 C−Si bond formation. *J. Am. Chem. Soc.* **2014**, *136*, 16780−16783. (b) Ding, F.; Zhang, Y.; Zhao, R.; Jiang, Y.; Bao, R. L.-Y.; Lin, K.; Shi, L. $B(C_6F_5)_3$-Promoted Hydrogenations of *N*-Heterocycles with Ammonia Borane. *Chem. Commun.* **2017**, *53*, 9262−9264. (c) Qiao, X.; Bao, Z.; Xing, H.; Yang, Y.; Ren, Q.; Zhang, Z. Organocatalytic Approach for Transfer Hydrogenation of Quinolines, Benzoxazines and Benzothiazines. *Catal. Lett.* **2017**, *147*, 1673−1678.

(4) (a) Lam, J.; Szkop, K. M.; Mosaferi, E.; Stephan, D. W. FLP Catalysis: Main Group Hydrogenations of Organic Unsaturated Substrates. *Chem. Soc. Rev.* **2019**, *48*, 3592−3612. (b) Scott, D. J.; Fuchter, M. J.; Ashley, A. E. Designing Effective 'Frustrated Lewis Pair' Hydrogenation Catalysts. *Chem. Soc. Rev.* **2017**, *46*, 5689−5700. (c) Scott, D. J.; Fuchter, M. J.; Ashley, A. E. Designing Effective 'Frustrated Lewis Pair' Hydrogenation Catalysts. *Chem. Soc. Rev.* **2017**, *46*, 5689−5700. (d) Stephan, D. W. Frustrated Lewis Pairs. *J. Am. Chem. Soc.* **2015**, *137*, 10018−10032. (e) Welch, G. C.; Stephan, D. W. Facile Heterolytic Cleavage of Dihydrogen by Phosphines and Boranes. *J. Am. Chem. Soc.* **2007**, *129*, 1880−1881. (f) Ullrich, M.; Lough, A. J.; Stephan, D. W. Reversible, Metal-Free, Heterolytic Activation of H_2 at Room Temperature. *J. Am. Chem. Soc.* **2009**, *131*, 52−53. (g) Sun, Q.; Daniliuc, C. G.; Bergander, K.; Kehr, G.; Erker, G. Carbon Monoxide Coupling Reactions via a Frustrated Lewis Pair-Derived η^2-Formyl Borane. *J. Am. Chem. Soc.* **2021**, *143*, 14992−14997. (h) Knaus, M. G.; Giuman, M. M.; Pothig, A.; Rieger, B. End of Frustration: Catalytic Precision Polymerization with Highly Interacting Lewis Pairs. *J. Am. Chem. Soc.* **2016**, *138*, 7776−7781. (i) Erös, G.; Nagy, K.; Mehdi, H.; Pápai, I.; Nagy, P.; Király, P.; Tárkányi, G.; Soós, T. Catalytic Hydrogenation with Frustrated Lewis Pairs: Selectivity Achieved by Size-Exclusion Design of Lewis Acids. *Chem.—Eur. J.* **2012**, *18*, 574−585. (j) Maier, A. F. G.; Tussing, S.; Schneider, T.; Flörke, U.; Qu, Z. W.; Grimme, S.; Paradies, J. Frustrated Lewis Pair Catalyzed Dehydrogenative Oxidation of Indolines and Other Heterocycles. *Angew. Chem., Int. Ed.* **2016**, *55*, 12219−12223. (k) Stephan, D. W.; Greenberg, S.; Graham, T. W.; Chase, P.; Hastie, J. J.; Geier, S. J.; Farrell, J. M.; Brown, C. C.; Heiden, Z. M.; Welch, G. C.; Ullrich, M. Metal-Free Catalytic Hydrogenation of Polar Substrates by Frustrated Lewis Pairs. *Inorg. Chem.* **2011**, *50*, 12338−12348. (l) Geier, S. J.; Chase, P. A.; Stephan, D. W. Metal-Free Reductions of *N*-Heterocycles via Lewis Acid Catalyzed Hydrogenation. *Chem. Commun.* **2010**, *46*, 4884−4886. (m) Wu, P.; Mao, H.; Chen, Z.; Cheng, L.; Wang, K. Controllable Reactivity Tuned by the Cooperativity in B/P and B/N Intermolecular Frustrated Lewis Pairs. *ChemCatChem.* **2022**, *14*, No. e202200895. (n) Wang, W.; Meng, W.; Du, H. $B(C_6F_5)_3$-Catalyzed Metal-Free Hydrogenation of 3,6-Diarylpyridazines. *Dalton Trans.* **2016**, *45*, 5945−5948. (o) Scott, D. J.; Fuchter, M. J.; Ashley, A. E. Metal-Free Hydrogenation Catalyzed by an Air-Stable Borane: Use of Solvent as a Frustrated Lewis Base. *Angew. Chem., Int. Ed.* **2014**, *53*, 10218−10222.

(5) (a) Li, B.; Wen, H. M.; Cui, Y.; Zhou, W.; Qian, G.; Chen, B. Emerging Multifunctional Metal−Organic Framework Materials. *Adv. Mater.* **2016**, *28*, 8819−8860. (b) Yuan, S.; Feng, L.; Wang, K.; Pang, J.; Bosch, M.; Lollar, C.; Sun, Y.; Qin, J.; Yang, X.; Zhang, P.; Wang, Q.; Zou, L.; Zhang, Y.; Zhang, L.; Fang, Y.; Li, J.; Zhou, H. C. Stable Metal−Organic Frameworks: Design, Synthesis, and Applications. *Adv. Mater.* **2018**, *30*, 1704303. (c) Jiang, J.; Yaghi, O. M. Brønsted Acidity in Metal−Organic Frameworks. *Chem. Rev.* **2015**, *115*, 6966−6997. (d) Corma, A.; García, H.; Xamena, F. Engineering Metal Organic Frameworks for Heterogeneous Catalysis. *Chem. Rev.* **2010**,

110, 4606−4655. (e) Zhou, H. C.; Kitagawa, S. Metal−Organic Frameworks (MOFs). *Chem. Soc. Rev.* **2014**, *43*, 5415−5418. (f) He, H.; Perman, J. A.; Zhu, G.; Ma, S. Metal-Organic Frameworks for CO_2 Chemical Transformations. *Small* **2016**, *12*, 6309−6324. (g) Liu, J.; Chen, L.; Cui, H.; Zhang, J.; Zhang, L.; Su, C. Y. Applications of Metalorganic Frameworks in Heterogeneous Supramolecular Catalysis. *Chem. Soc. Rev.* **2014**, *43*, 6011−6061.

(6) (a) Jiang, H.; Zhang, W.; Kang, X.; Cao, Z.; Chen, X.; Liu, Y.; Cui, Y. Topology-Based Functionalization of Robust Chiral Zr-Based Metal−Organic Frameworks for Catalytic Enantioselective Hydrogenation. *J. Am. Chem. Soc.* **2020**, *142*, 9642−9652. (b) Wang, Y.; Huang, N. Y.; Shen, J. Q.; Liao, P. Q.; Chen, X. M.; Zhang, J. P. Hydroxide Ligands Cooperate with Catalytic Centers in Metal−Organic Frameworks for Efficient Photocatalytic CO_2 Reduction. *J. Am. Chem. Soc.* **2018**, *140*, 38−41. (c) Li, F. L.; Shao, Q.; Huang, X.; Lang, J. P. Nanoscale Trimetallic Metal−Organic Frameworks Enable Efficient Oxygen Evolution Electrocatalysis. *Angew. Chem., Int. Ed.* **2018**, *57*, 1888−1892. (d) Fei, H.; Cohen, S. M. Metalation of a Thiocatechol-Functionalized Zr(IV)-Based Metal−Organic Framework for Selective C−H Functionalization. *J. Am. Chem. Soc.* **2015**, *137*, 2191−2194. (e) Zeng, L.; Wang, Z.; Wang, Y.; Wang, J.; Guo, Y.; Hu, H.; He, X.; Wang, C.; Lin, W. Photoactivation of Cu Centers in Metal−Organic Frameworks for Selective CO_2 Conversion to Ethanol. *J. Am. Chem. Soc.* **2020**, *142*, 75−79. (f) Zhou, T. Y.; Auer, B.; Lee, S. J.; Telfer, S. G. Catalysts Confined in Programmed Framework Pores Enable New Transformations and Tune Reaction Efficiency and Selectivity. *J. Am. Chem. Soc.* **2019**, *141*, 1577−1582. (g) Manna, K.; Ji, P.; Greene, F. X.; Lin, W. Metal−Organic Framework Nodes Support Single-Site Magnesium−Alkyl Catalysts for Hydroboration and Hydroamination Reactions. *J. Am. Chem. Soc.* **2016**, *138*, 7488−7491. (h) Burgess, S. A.; Kassie, A.; Baranowski, S. A.; Fritzsching, K. J.; Schmidt-Rohr, K.; Brown, C. M.; Wade, C. R. Improved Catalytic Activity and Stability of a Palladium Pincer Complex by Incorporation into a Metal−Organic Framework. *J. Am. Chem. Soc.* **2016**, *138*, 1780−1783. (i) Liu, X. H.; Ma, J. G.; Niu, Z.; Yang, G. M.; Cheng, P. An Efficient Nanoscale Heterogeneous Catalyst for the Capture and Conversion of Carbon Dioxide at Ambient Pressure. *Angew. Chem., Int. Ed.* **2015**, *54*, 988−991. (j) Ye, J.; Johnson, J. K. Design of Lewis Pair-Functionalized Metal Organic Frameworks for CO_2 Hydrogenation. *ACS Catal.* **2015**, *5*, 2921−2928. (k) Zhang, W.; Nafady, A.; Shan, C.; Wojtas, L.; Chen, Y.-S.; Cheng, Q.; Zhang, X. P.; Ma, S. Functional Porphyrinic Metal-Organic Framework as a New Class of Heterogeneous Halogen Bond Donor Catalyst. *Angew. Chem. Int. Ed.* **2021**, *60*, 24312−24317. (l) Wang, Q.; Yang, G.; Fu, Y.; Li, N.; Hao, D.; Ma, S. Nanospace Engineering of Metal-Organic Frameworks for Heterogeneous Catalysis. *ChemNanoMater.* **2022**, No. e202100396.

(7) (a) Yu, X.; Cohen, S. M. Photocatalytic Metal−Organic Frameworks for Selective 2,2,2-Trifluoroethylation of Styrenes. *J. Am. Chem. Soc.* **2016**, *138*, 12320−12323. (b) Gong, W.; Chen, X.; Jiang, H.; Chu, D.; Cui, Y.; Liu, Y. Highly Stable Zr(IV)-Based Metal−Organic Frameworks with Chiral Phosphoric Acids for Catalytic Asymmetric Tandem Reactions. *J. Am. Chem. Soc.* **2019**, *141*, 7498−7508. (c) Noh, H.; Cui, Y.; Peters, A. W.; Pahls, D. R.; Ortuno, M. A.; Vermeulen, N. A.; Cramer, C. J.; Gagliardi, L.; Hupp, J. T.; Farha, O. K. An Exceptionally Stable Metal−Organic Framework Supported Molybdenum (VI) Oxide Catalyst for Cyclohexene Epoxidation. *J. Am. Chem. Soc.* **2016**, *138*, 14720−14726. (d) Huang, G.; Yang, Q.; Xu, W.; Yu, S. H.; Jiang, H. L. Polydimethylsiloxane Coating for a Palladium/MOF Composite: Highly Improved Catalytic Performance by Surface Hydrophobization. *Angew. Chem., Int. Ed.* **2016**, *55*, 7379−7383. (e) Hackler, R. A.; Pandharkar, R.; Ferrandon, M. S.; Kim, I. S.; Vermeulen, N. A.; Gallington, L. C.; Chapman, K. W.; Farha, O. K.; Cramer, C. J.; Sauer, J.; Gagliardi, L.; Martinson, A. B. F.; Delferro, M. Isomerization and Selective Hydrogenation of Propyne: Screening of Metal−Organic Frameworks Modified by Atomic Layer Deposition. *J. Am. Chem. Soc.* **2020**, *142*, 20380−20389. (f) Zhao, M.; Yuan, K.; Wang, Y.; Li, G.; Guo, J.; Gu, L.; Hu, W.; Zhao, H.; Tang, Z. Metalorganic Frameworks as Selectivity Regulators for Hydrogenation Reactions. *Nature* **2016**, *539*, 76−80. (g) Saha, S.; Das, G.; Thote, J.; Banerjee, R. Photocatalytic Metal−Organic Framework from CdS Quantum Dot Incubated Luminescent Metallohydrogel. *J. Am. Chem. Soc.* **2014**, *136*, 14845−14851. (h) Ma, X.; Liu, H.; Yang, W.; Mao, G.; Zheng, L.; Jiang, H. L. Modulating Coordination Environment of Single-Atom Catalysts and Their Proximity to Photosensitive Units for Boosting MOF Photocatalysis. *J. Am. Chem. Soc.* **2021**, *143*, 12220−12229. (i) Qi, L.; Chen, J.; Zhang, B.; Nie, R.; Qi, Z.; Kobayashi, T.; Bao, Z.; Yang, Q.; Ren, Q.; Sun, Q.; Zhang, Z.; Huang, W. Deciphering a Reaction Network for the Switchable Production of Tetrahydroquinoline or Quinoline with MOF-Supported Pd Tandem Catalysts. *ACS Catal.* **2020**, *10*, 5707−5714. (j) Zhao, Y.; Qi, S.; Niu, Z.; Peng, Y.; Shan, C.; Verma, G.; Wojtas, L.; Zhang, Z.; Zhang, B.; Feng, Y.; Chen, Y. S.; Ma, S. Robust Corrole-Based Metal−Organic Frameworks with Rare 9-Connected Zr/Hf-Oxo Clusters. *J. Am. Chem. Soc.* **2019**, *141*, 14443−14450. (k) Deria, P.; Mondloch, J. E.; Tylianakis, E.; Ghosh, P.; Bury, W.; Snurr, R. Q.; Hupp, J. T.; Farha, O. K. Perfluoroalkane Functionalization of NU-1000 via Solvent-Assisted Ligand Incorporation: Synthesis and CO_2 Adsorption Studies. *J. Am. Chem. Soc.* **2013**, *135*, 16801−16804. (l) Rayder, T. M.; Bensalah, A. T.; Li, B.; Byers, J. A.; Tsung, C. K. Engineering Second Sphere Interactions in a Host−Guest Multicomponent Catalyst System for the Hydrogenation of Carbon Dioxide to Methanol. *J. Am. Chem. Soc.* **2021**, *143*, 1630−1640.

(8) (a) Shyshkanov, S.; Nguyen, T. N.; Chidambaram, A.; Stylianou, K. C.; Dyson, P. J. Frustrated Lewis Pair-Mediated Fixation of CO_2 within a Metal−Organic Framework. *Chem. Commun.* **2019**, *55*, 10964−10967. (b) Shyshkanov, S.; Nguyen, T. N.; Ebrahim, F. M.; Stylianou, K. C.; Dyson, P. J. In Situ Formation of Frustrated Lewis Pairs in a Water-Tolerant Metal-Organic Framework for the Transformation of CO_2. *Angew. Chem., Int. Ed.* **2019**, *58*, 5371−5375. (c) Niu, Z.; Bhagya-Gunatilleke, W. D. C.; Sun, Q.; Lan, P. C.; Perman, J.; Ma, J. G.; Cheng, Y.; Aguila, B.; Ma, S. Metal-Organic Framework Anchored with a Lewis Pair as a New Paradigm for Catalysis. *Chem.* **2018**, *4*, 2587−2599. (d) Zhang, Y.; Lan, P. C.; Martin, K.; Ma, S. Porous Frustrated Lewis Pair Catalysts: Advance and Perspective. *Chem. Catal.* **2022**, *2*, 439−457. (e) Zhang, Y.; Chen, S.; Al-Enizi, A. M.; Nafady, A.; Tang, Z.; Ma, S. Chiral Frustrated Lewis Pair@Metal-Organic Framework as a New Platform for Heterogeneous Asymmetric Hydrogenation. *Angew. Chem. Int. Ed.* **2022**, *61*, No. e202213399.

(9) Niu, Z.; Zhang, W.; Lan, P. C.; Aguila, B.; Ma, S. Promoting Frustrated Lewis Pairs for Heterogeneous Chemoselective Hydrogenation via the Tailored Pore Environment within Metal−Organic Frameworks. *Angew. Chem., Int. Ed.* **2019**, *58*, 7420−7424.

(10) (a) Dunning, S. G.; Nandra, G.; Conn, A. D.; Chai, W.; Sikma, R. E.; Lee, J. S.; Kunal, P.; Reynolds, J. E., III; Chang, J.-S.; Steiner, A.; Henkelman, G.; Humphrey, S. M. A Metal−Organic Framework with Cooperative Phosphines That Permit Post-Synthetic Installation of Open Metal Sites. *Angew. Chem., Int. Ed.* **2018**, *57*, 9295−9299. (b) Sawano, T.; Lin, Z.; Boures, D.; An, B.; Wang, C.; Lin, W. Metal−Organic Frameworks Stabilize Mono(phosphine)−Metal Complexes for Broad-Scope Catalytic Reactions. *J. Am. Chem. Soc.* **2016**, *138*, 9783−9786. (c) Madrahimov, S. T.; Gallagher, J. R.; Zhang, G.; Meinhart, Z.; Garibay, S. J.; Delferro, M.; Miller, J. T.; Farha, O. K.; Hupp, J. T.; Nguyen, S. T. Gas-Phase Dimerization of Ethylene under Mild Conditions Catalyzed by MOF Materials Containing (bpy)Ni^{II} Complexes. *ACS Catal.* **2015**, *5*, 6713−6718. (d) Drake, T.; Ji, P.; Lin, W. Site Isolation in Metal−Organic Frameworks Enables Novel Transition Metal Catalysis. *Acc. Chem. Res.* **2018**, *51*, 2129−2138. (e) Sikma, R. E.; Cohen, S. M. Metal−Organic Frameworks with Zero and Low-Valent Metal Nodes Connected by Tetratopic Phosphine Ligands. *Angew. Chem., Int. Ed.* **2022**, *61*, No. e202115454. (f) Yasui, S.; Tojo, S.; Majima, T. Reaction of Triarylphosphine Radical Cations Generated from Photoinduced Electron Transfer in the Presence of Oxygen. *J. Org. Chem.* **2005**, *70*, 1276−1280.

(11) (a) Liu, J.; Li, Z.; Zhang, X.; Otake, K.; Zhang, L.; Peters, A. W.; Young, M. J.; Bedford, N. M.; Letourneau, S. P.; Mandia, D. J.;

https://doi.org/10.1021/jacs.3c04929
J. Am. Chem. Soc. 2023, 145, 14994−15000

Elam, J. W.; Farha, O. K.; Hupp, J. T. Introducing Nonstructural Ligands to Zirconia-like Metal−Organic Framework Nodes to Tune the Activity of Node-Supported Nickel Catalysts for Ethylene Hydrogenation. *ACS Catal.* **2019**, *9*, 3198−3207. (b) Li, X.; Yu, J.; Lu, Z.; Duan, J.; Fry, H. C.; Gosztola, D. J.; Maindan, K.; Rajasree, S. S.; Deria, P. Photoinduced Charge Transfer with a Small Driving Force Facilitated by Exciplex-Like Complex Formation in Metal−Organic Frameworks. *J. Am. Chem. Soc.* **2021**, *143*, 15286−15297. (c) Islamoglu, T.; Goswami, S.; Li, Z.; Howarth, A. J.; Farha, O. K.; Hupp, J. T. Postsynthetic Tuning of Metal−Organic Frameworks for Targeted Applications. *Acc. Chem. Res.* **2017**, *50*, 805−813. (d) Wang, T. C.; Vermeulen, N. A.; Kim, I. S.; Martinson, A. B. F.; Stoddart, J. F.; Hupp, J. T.; Farha, O. K. Scalable Synthesis and Post-Modification of a Mesoporous Metal-Organic Framework Called NU-1000. *Nat. Protoc.* **2016**, *11*, 149−162. (e) Deria, P.; Mondloch, J. E.; Tylianakis, E.; Ghosh, P.; Bury, W.; Snurr, R. Q.; Hupp, J. T.; Farha, O. K. Perfluoroalkane Functionalization of NU-1000 via Solvent-Assisted Ligand Incorporation: Synthesis and CO_2 Adsorption Studies. *J. Am. Chem. Soc.* **2013**, *135*, 16801−16804.

(12) (a) Etter, M. C. Encoding and Decoding Hydrogen-Bond Patterns of Organic Compounds. *Acc. Chem. Res.* **1990**, *23*, 120−126. (b) Karamzadeh, S.; Sanchooli, E.; Oveisi, A. R.; Daliran, S.; Luque, R. Visible-LED-Light-Driven Photocatalytic Synthesis of N-Heterocycles Mediated by a Polyoxometalate-Containing Mesoporous Zirconium Metal-Organic Framework. *Appl. Catal. B Environ.* **2022**, *303*, 120815. (c) Quan, Y.; Lan, G.; Fan, Y.; Shi, W.; You, E.; Lin, W. Metal−Organic Layers for Synergistic Lewis Acid and Photoredox Catalysis. *J. Am. Chem. Soc.* **2020**, *142*, 1746−1751.

https://doi.org/10.1021/jacs.3c04929
J. Am. Chem. Soc. 2023, 145, 14994−15000